J. Phys. Chem. **1996,** *100,* 17855−17861 **17855**

Reaction Modulation Spectoscopy: A New Approach to Quantifying Reaction Mechanisms[†]

Neil M. Donahue,* Kenneth L. Demerjian,[‡] and James G. Anderson

Department of Chemistry, Harvard University, Cambridge, Massachusetts 02138

Received: May 13, 1996; In Final Form: September 3, 1996[⊗]

We report a new experimental method, *reaction modulation spectroscopy*, (RMS), that shows great promise in enabling the systematic analysis of complicated oxidation mechanisms over the full range of atmospheric pressures and temperatures. The method is a form of difference spectroscopy in which we employ FTIR absorption spectroscopy in a high-pressure flow system (HPFS) where a plume of reacting species is examined before any significant fraction reaches the tube wall. The onset of the reaction is modulated by modulating the flow of an initiating radical species over a period that is short compared to any associated with experimental drifts. Spectra obtained with the radical source on and off are ratioed, giving a transmittance spectrum showing only the effects of the reaction modulation. The system is in a steady state, so signal averaging over long periods (up to several days) may be employed, if necessary, to obtain a high signal-to-noise ratio. Because no bulk reagents are disturbed in the process, we observe extremely precise conservation of mass in the reaction plume. We illustrate the technique for the system $OH + C_3F_6$ ($+ O_2$, NO_x, ...) $\rightarrow\rightarrow CF_2O +$ CF_3CFO, where we observe nearly 100% conservation of odd-nitrogen species and roughly 90% conservation of carbon under conditions chosen to force the reaction to completion, with residual spectra consistent with unidentified minor products having cross sections similar to the observed aldehydes.

Introduction

Fourier transform spectroscopy (FTS) has been used for decades to characterize atmospheric oxidation mechanisms of many chemical species.[1] It has the obvious advantage of offering selective detection of almost all atmospheric trace species, the only exceptions being symmetric diatomic and atomic species. However, the technique is most often coupled to a smog chamber, where radicals are generated continuously by a photolytic mechanism and the development of reactant and product concentrations is monitored over time. Although such an approach is straightforward, it suffers in several respects: (1) the chemical systems develop over long times, often several hours, and many species have ample time to interact with the walls of the chamber; (2) short lived radical species are not observed because they will be in a photochemical steady state at very low concentrations; (3) even moderately unreactive reaction products will be subject to oxidation by the radicals responsible for the initial oxidation reaction; (4) because the system is developing over time, the relatively low sensitivity of FT measurements often forces experiments to be run with correspondingly high radical concentrations, which in turn increase the risk that secondary radical reactions perturb the observed chemistry; (5) large systems designed to reduce the surface area to volume ratio are difficult to operate at pressures and temperatures different from the those of the laboratory in which they reside. Despite these difficulties, we owe much of our understanding of atmospheric oxidation mehanisms to these systems.

A second approach is to measure absolute rate constants and branching ratios for a coupled set of concerted reactions. A difficulty with this approach is that absolute rate constants are most often measured on systems with highly sensitive but highly specific detection methods optimized for particular radicals. Although this is ideal for determining rate constants, the techniques are generally difficult to calibrate and restrict the investigator to a small set of observable species. This makes these techniques less desirable for determining branching ratios and identifying unknown products of reactions. Furthermore, unless the individual rate constant measurements are accompanied by experiments constraining the overall mechanism, errors will propagate and will overwhelm any attempt to quantify that mechanism based on the individual measurements.

We report here a method that bridges these two approaches. We use FT absorption spectroscopy to probe a reactive plume in a high-pressure flow kinetics system (HPFS) designed to measure absolute rate constants over the entire range of pressures and temperatures encountered in the atmosphere. The plume is probed before it reaches the flow system wall, thus completely eliminating any potential wall effects. The plume is in an advective chemical steady state, so different stages of the reaction are spread out in space but remain effectively constant in time over long periods. This permits the observation of intermediate radical species and helps to prevent the interaction of radicals that appear at different stages of a mechanism. The stability over time permits signal averaging to overcome the poor sensitivity of the FT measurements.

To impose an ac signal on the experiment, we modulate the onset of a reaction in our system by alternately turning on and off the flow of a radical precursor without changing any other experimental conditions (i.e., the concentrations of other reagents). For this reason, we call the technique reaction modulation spectroscopy (RMS). The reaction modulation has two profound effects: it allows us to directly generate difference spectra of the change in reactant and product abundances caused by the introduction of a radical; it imposes strict conservation of mass on the experiment. This greatly enhances our ability to quantify the branching ratios of individual reactions and overall mechanisms.

The RMS technique extends the molecular modulation spectrometry (MMS) technique developed by Johnston in the late 1960s,[2] which was used extensively to study radical

---

[†] This paper is dedicated to the memory of Hiromi Niki.

* To whom correspondence should be addressed.

[‡] Also at Department of Atmospheric Sciences, State University of New York, Albany, New York.

[⊗] Abstract published in *Advance ACS Abstracts,* October 15, 1996.

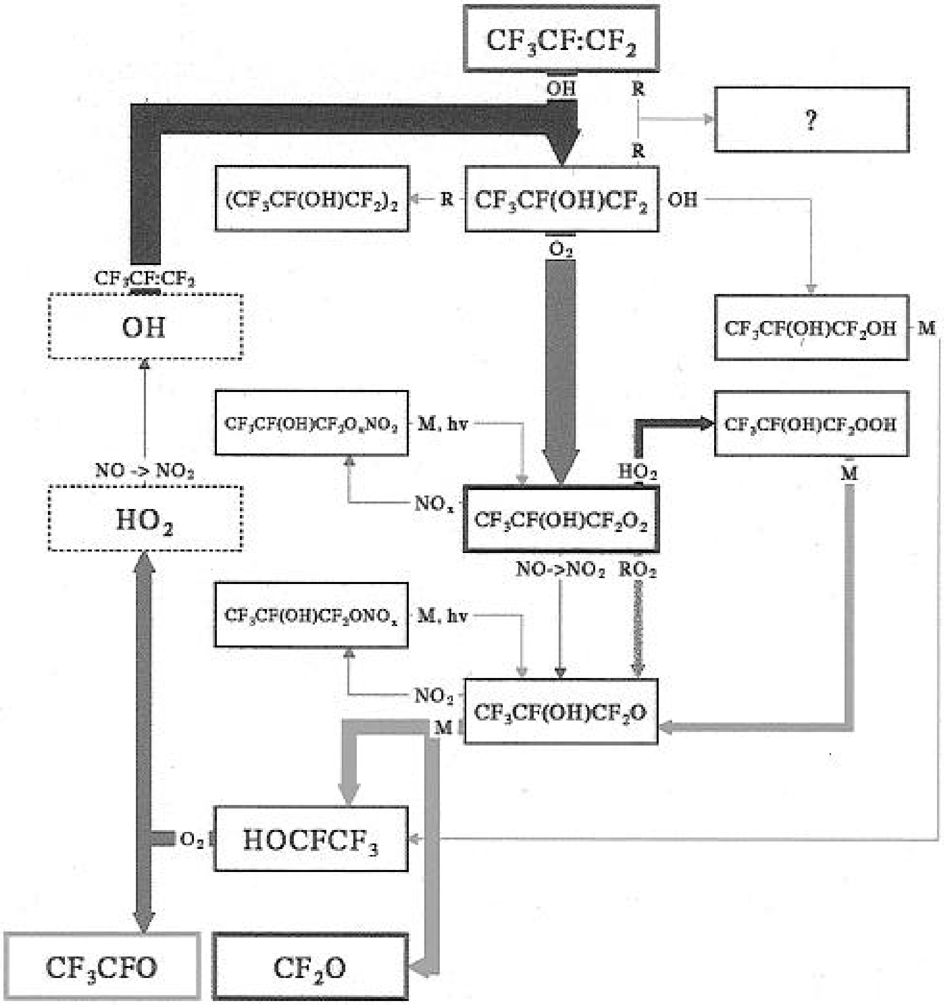

Figure 1. Possible oxidation mechanism for C_3F_6 + OH → products under low NO_x conditions. Arrow sizes are proportional to peak reaction fluxes. Arrow colors indicate reagent families: green is oxygen, blue is NO_x, and red is thermal decomposition. The production of two aldehydes, CF_2O and CF_3CFO, is likely.

intermediates in flash photolysis systems.[3,4] The major differences between RMS and MMS are the use of an FT spectrometer in place of a dispersive spectrometer, which permits more precise collection of modulated spectra, and the application of the modulation technique to a flow system, as opposed to a flash photolysis system, which permits us to exploit a rapidly established advective−chemical steady state to examine any time in the reaction sequence. The MMS technique typically involves monitoring the amplitude and phase shift of an ac signal produced in a system where the chemical time scales are similar to the modulation period.[2] The RMS technique separates the period of modulation from the chemical time scales by exploiting the advective−chemical steady state inherent in a flow tube. The absorption path is oriented perpendicular to the flow direction, isolating a particular reaction time. The chemical time scales under exploration are generally on the order of 100 ms, while the modulation period is typically 5 min. Scanning is nearly continuous, with only short pauses (10% or less of the total) required for the advective−chemical steady state to be established when the radical source is modulated.

Test Mechanism

To test the RMS technique, we chose the chemical system OH + C_3F_6 (+ O_2, NO_x, ...) →→ CF_2O + CF_3CFO, which is graphically presented in Figure 1. The rate constant at 298K is 2.1×10^{-12} cm^3 $molecule^{-1}$ s^{-1}.[5] We chose C_3F_6 for two reasons: as an unsaturated hydrocarbon, it represents a general class of compounds of great atmospheric importance and as a fluorinated species, it presents us with compounds whose IR absorption cross sections are large and generally well-known.

This reaction has also been used recently as an OH scrubber in atmospheric laser-induced fluorescence measurements in order to test for generation of OH by the UV laser.[5,6] Reaction channels that rapidly regenerate OH radicals upon the introduction of such a scrubber could diminish its effectiveness. These same regeneration mechanisms could also produce systematic errors in kinetics measurements of OH−alkene reactions, which are notoriously difficult.[7,8]

Figure 1 portrays the oxidation of C_3F_6 under low-NO_x conditions. This mechanism is consistent with the general paradigm for hydrocarbon oxidation.[9] It is also consistent with the data presented in this work, though much more work is yet required to fully constrain the mechanism. Each box in the figure represents a different species, and the connecting arrows represent the reactive fluxes between the species. The size of each arrow is proportional to the magnitude of each reactive flux. The color of each arrow identifies the other chemical family interacting with the hydrocarbon at each stage: green represents oxygen, blue NO_x, and red thermal decomposition. Colored boxes identify species appearing in spectra in this paper. The reference spectra for such species will be plotted in the same color.

In the sequence depicted here, OH radicals add to the central carbon, forming a radical that rapidly combines with oxygen to produce a peroxy radical. In the absence of NO_x, this radical will react with other peroxy radicals along several possible pathways, often eventually producing a substituted alkoxy radical. For large and highly substituted hydrocarbons these alkoxy radicals may decompose into an aldehyde and an unstable radical, which in turn may rapidly react with oxygen to produce a second aldehyde and the hydroperoxy radical, HO_2. If NO_x were present in sufficient quantity, the alkoxy radical or an organic nitrate would be produced, and HO_2 would be rapidly converted to OH, closing a catalytic hydrocarbon oxidation cycle. A parallel sequence, with OH addition to the terminal carbon, yields the identical aldehydes. We therefore expect that, under the proper conditions, we should be able to force the system to produce one of each of the two aldehydes for every C_3F_6 removed.

Experimental Method

All the experiments described here were conducted on our high-pressure flow system (HPFS). The system has been extensively described in the literature,[10,11] so we shall describe only the capabilities specific to the RMS technique.

Reaction modulation spectroscopy (RMS) is conceptually straightforward. We exploit several attributes of the HPFS to achieve very high sensitivity to the disappearance of reactants and appearance of reaction products while guaranteeing conservation of material in the sampling volume. We observe the radical plume with FTIR absorption spectroscopy in a White cell located roughly 50 cm downstream of the radical source. Reagents other than the radical (e.g., a hydrocarbon, O_2, NO, NO_2) are well mixed in the carrier flow. The carrier gas and reagents are not recirculated in this experiment; they pass once through the reaction zone and are pumped out of the system. The flow out of the radical source is a tiny fraction ($\sim$1%) of the carrier flow, so the reagents immediately mix into the radical plume, though the plume itself spreads only slowly toward the flow tube wall. In the White cell, the plume is a Gaussian of roughly 2 cm half width. Thus, essentially none of the radical has reached the wall at 6 cm radius.

The experiment is in a steady state; all flows are controlled with mass flow controllers, and very little surface area requires any conditioning. Practice has shown that the system will remain stable for days; reagent concentrations maintained by flow controllers drift by a few percent or less per day, while radical concentrations typically drift by roughly 10% per day. The White cell is placed so that it examines a volume element located roughly 100 ms into the reaction sequence (for a 500 cm/s flow). We generally tailor the conditions so that the initial reaction will go to completion in 10 ms or less, leaving reaction products equal in abundance to the initial radical abundance. The excess reagent concentration will have dropped by an amount equal to the amount of radical removed, assuming that no secondary reactions involve the initial reagent. However, this will generally be only a small fraction of the total excess reagent concentration.

Our goal is to identify products of the initial reaction and succeeding fast reactions and to quantify the branching of the overall mechanism. The sample volume has not come into contact with the flow tube wall, and very little diffusion has occurred (and that has little or no dependence on mass under most experimental conditions, where turbulent diffusion dominates). We therefore expect the sample volume to contain products of the gas phase reaction exactly equal to (within a few percent or less) the quantity of reagents consumed. Quantification of reactants and products observed with the FT spectrometer requires knowledge of only their relative cross sections, since the sample volumes for all species are identical; however, companion LIF and RF measurements can provide vital additional information, especially for atoms, which of course do not absorb in the IR, and OH, which has a very small integrated cross section.

To exploit the steady state concentrations in the HPFS without losing sensitivity because of base line drifts in the FTIR, we modulate the concentration of the intiating radical by modulating the flow of a radical precursor in the radical source. For instance, in the most common source of OH radicals we dissociate H_2 in a microwave-induced plasma (MIP) and then titrate the resulting hydrogen atoms with NO_2, producing OH and NO:

$$H_2 \rightarrow H + H$$

$$H + NO_2 \rightarrow OH + NO \tag{1}$$

In this case, the OH is modulated by modulating the (tiny) flow of H_2.

Spectra are taken and coadded during each phase of the radical modulation cycle. The two "offline" spectra surrounding an "online" spectrum are then averaged to produce a background spectrum, and the ratio of the two gives a transmittance spectrum showing directly any changes in absorption caused by the modulation of the radical. This is the most important aspect of the RMS technique: we directly record the change in abundance of all species, including the excess reagent. There is no spectral subtraction to be performed; the spectra may be directly analyzed to quantify the reaction. Any number of these transmittance spectra may be averaged to increase the signal-to-noise ratio (S/N); the minimum noise level observed to date, on a two-day experiment, corresponded to an optical depth of roughly 10^{-6} at 4 cm^{-1} resolution.

To optimize the S/N for the several species being measured, we often collect spectra at more than one resolution during each cycle. Sampling resolutions are generally matched to the coherence length of the resolvable portion of a given spectrum. Where rotational transitions can be resolved, this is generally the highest resolution of the instrument. Where the spacing is too narrow or nonexistant, 8 cm^{-1} is often optimal.

Data Analysis

Data are collected with and without the initating radical. The resulting spectra are then divided to give a transmittance, which is in turn converted into an optical depth,

$$\tau_\nu = \ln(I_{\nu,\mathrm{off}}/I_{\nu,\mathrm{on}}) \tag{2}$$

where τ_ν is the optical depth as a function of wavenumber and I_ν is the observed spectrum. Provided that either features in the spectrum are well resolved by the spectrometer or that the concentrations of all absorbing species are small enough for the actual absorption of sharp features to be small (<20%), this observed optical depth may be simply related to the absorption cross sections of all constituents in the path of the spectrometer.

$$\tau_\nu = \sum_j L\sigma_{j,\nu}C_j + N_\nu \tag{3}$$

where L is the absorption path length, $\sigma_{j,\nu}$ is the cross section of species j as a function of wavenumber, C_j is the number densitiy of species j, and N_ν is a wavenumber dependent noise term. We may freely multiply each side of eq 3 by an arbitrary function. We choose $\sigma_{i,\nu}$, the cross section of a species i, whose column abundance we wish to determine:

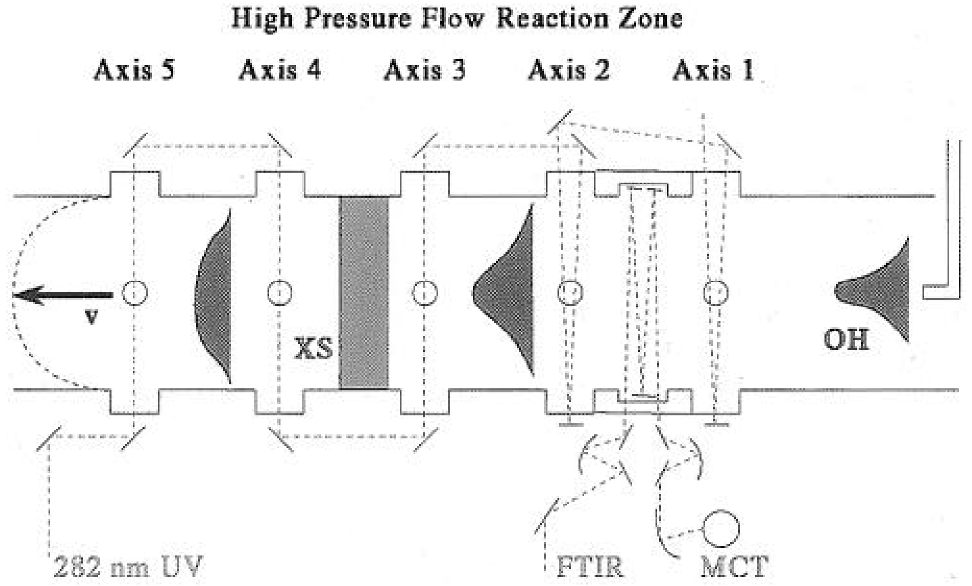

Figure 2. High-pressure flow system reaction zone. The tube is 6.3 cm in radius, and the section shown is ~150 cm long. The carrier flow (N_2) is from right to left (blue curve and vector at left). Pressure ranges from 1 to 1000 Torr, and temperature ranges from 180 to 400 K. Reagents other than the radical are well mixed in the carrier flow (i.e., cyan stripe). The radical is generated in a sidearm and injected into the core of the flow with a thin quartz tube. Radicals are measured with LIF (OH, five axes shown) or atomic RF (Cl, H, O, axes not shown, between LIF axes) in the core of the flow (black circles). A 44-pass, 6 in. base path White cell sits between the first and second LIF axes, oriented across the spreading radical plume. The White cell is coupled to a 0.25 cm^{-1} FTIR spectrometer (Mattson RS1). A typical radical plume is sketched in green, with the height of each green curve above each base line representing concentration. This curve is for low reactivity. With high reagent concentration, essentially all radicals would be removed by the White cell.

$$\sigma_{i,\nu}\tau_\nu = \sum_j L\sigma_{i,\nu}\sigma_{j,\nu}C_j + \sigma_{i,\nu}N_\nu \qquad (4)$$

This serves as an integrating factor and allows us to solve for the scalar column abundance by integrating over all wavenumbers (the integration is implied by the repeating subscripts):

$$LC_i = \frac{\sigma_{i,\nu}\tau_\nu}{\sigma_{i,\nu}\sigma_{i,\nu}} - \sum_{j\neq i}\frac{\sigma_{i,\nu}\sigma_{j,\nu}}{\sigma_{i,\nu}\sigma_{i,\nu}}LC_\mathrm{j} - \frac{\sigma_{i,\nu}N_\nu}{\sigma_{i,\nu}\sigma_{i,\nu}} \qquad (5)$$

We are finding the correlation coefficient of a reference spectrum with our data (τ_ν) and correcting for the covariance between the reference spectrum and the spectra of other features present in the data. The data and reference spectra should be scaled to the (slowly varying) observed noise for proper quantitative analysis. However, the noise is roughly constant over most of the range used in this work, so this refinement has not yet been implemented.

Equation 5 allows us to simultaneously solve for the abundance of all species in the data, but because of the coupling, the approach will be iterative. We turn eq 5 into an iterator by adding a gain, G, to the coupling term.

$$LC_i = \frac{\sigma_{i,\nu}\tau_\nu}{\sigma_{i,\nu}\sigma_{i,\nu}} - G\sum_{j\neq i}\frac{\sigma_{i,\nu}\sigma_{j,\nu}}{\sigma_{i,\nu}\sigma_{i,\nu}}LC_\mathrm{j} - \frac{\sigma_{i,\nu}N_\nu}{\sigma_{i,\nu}\sigma_{i,\nu}} \qquad (6)$$

The gain is generally kept less than 1 (we use 1/2) to improve the stability of the iteration. In practice, the correlation between the reference spectrum and the noise is assumed to be zero. We repeatedly subtract the observed levels of the various compounds from the data and analyze the residual spectrum for remaining signal until no more signal is found.

As part of the analysis procedure, we may apply high- and low-pass filters to the data and the reference spectra. This is done in the transformed (retardation) space. The low-pass filter (apodization) is often simply the maximum optical path difference of the interferometer, which determines the resolution. The high-pass filter is chosen to minimize the error in the procedure. Its main function is to reduce the noise dependent term, $\sigma_{i,\nu}N_\nu$. For the work described in this paper, we low-pass filter at 128 cm^{-1}, which effectively eliminates the influence of base line drifts and curvature while passing most of the information about the reference spectra. One may apply different high- and low-pass filters for each compound, though the algorithm is slightly more complicated. Species that exhibit sharp, rotationally resolved features (i.e., small species with small moments of intertia) often benefit from aggressive high-pass filtering, which produces a "gap" function.[12] Filtering in the wavenumber regime is also often necessary; when unidentified features are present in the data, they must be masked out before analyzing for other species if there is significant correlation.

Once optimal concentrations have been determined for the suite of reference compounds, we are left with a residual spectrum equal to the noise term. We can then assess the uncertainty in the derived concentrations by analyzing the noise spectrum for the presence of each species at a series of locations slightly offset from the location of the true spectral features. Assuming that the noise varies only slowly with wavenumber, we find the correlation of each reference spectrum with the residual spectrum, offset over a range of wavenumbers, λ. The root-mean-square of this lag spectrum is taken to be the uncertainty of the measurement.

$$\delta LC_i = \frac{1}{\sigma_{i,\nu}\sigma_{i,\nu}}\frac{1}{2\Delta\lambda}\left(\int_{-\Delta\lambda}^{+\Delta\lambda}(\sigma_{i(\nu-\lambda)}N_\nu)^2\,\mathrm{d}\lambda\right)^{1/2} \qquad (7)$$

Results

A sample RMS spectrum at 1 cm^{-1} resolution for the reaction $OH + C_3F_6 \rightarrow\rightarrow CF_2O + CF_3CFO$ is shown in Figure 3. The experiment was performed at 9 Torr and 300 K in a 652 cm s^{-1} flow of nitrogen. The White cell sits some 50 cm downstream from the radical source, so the reaction time under study was roughly 0.1 s, though plume mixing makes this time imprecise. The carrier flow was augmented with 3×10^{14}

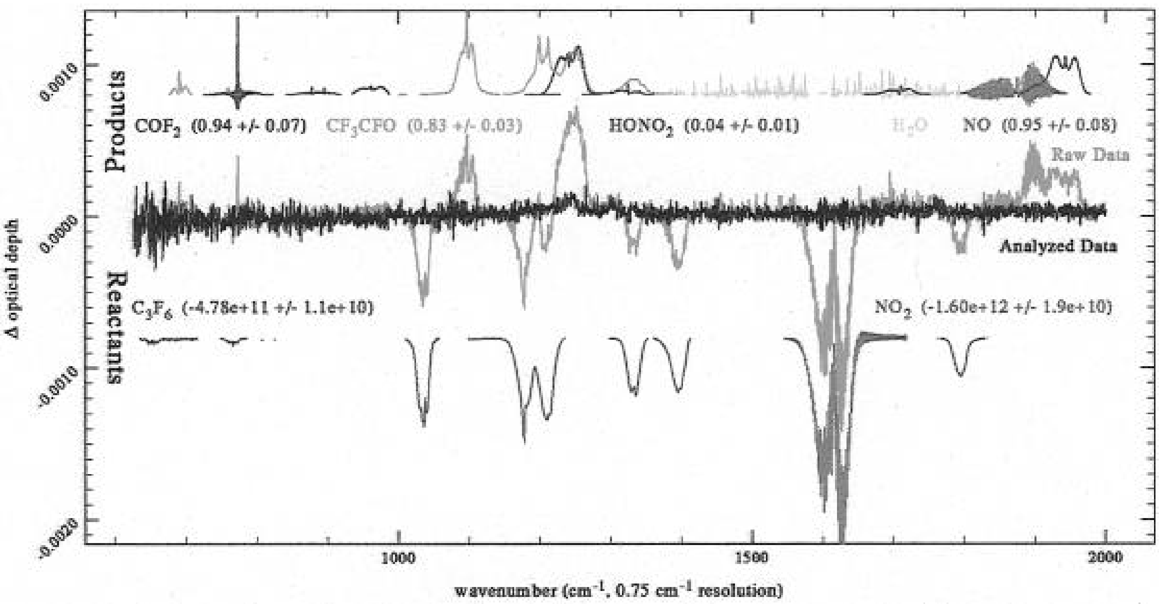

Figure 3. Reaction modulation spectrum for OH + C_3F_6 → products. The abscissa is the change in optical depth between spectra taken with the OH on and off. Reactants appear with negative optical depths, while products appear with positive optical depths. The raw spectra are plotted in red. Spectra for observed species are plotted in various colors below (reactants) and above (products) the raw data, scaled to the quantity observed. The result of subtracting the observed species from the raw data is then plotted in black. The number density of the C_3F_6 removed is shown, while the ratio to this number is shown for the aldehydes. Roughly 90% of the reaction is explained, and the residual spectrum is consistent with an unidentified product present at the 10% level. Likewise, the number density of NO_2 removed is shown, along with the ratios of the observed NO and $HONO_2$ to this number. NO_x is conserved within experimental error.

molecules cm^{-3} O_2 and 1 × 10^{13} molecules cm^{-3} NO to force the mechanism depicted in Figure 1 to completion. The initial C_3F_6 concentration was 5.5 × 10^{13} molecules cm^{-3}, while the initial OH concentration was approximately 3 × 10^{11} molecules cm^{-3}, produced with the source described by reaction 1. The OH lifetime was thus approximately 0.01 s. Spectra were collected over 5 h, using an MCT detector. Figure 3 shows the change in optical depth caused by the modulation of the OH radical source. It is the direct result of the averaging discussed above; no spectral subtraction to remove large reagent signals is needed.

All species whose abundance drops when the radical source is turned on appear with negative optical depths in the spectra; all products appear with positive optical depths. The raw data are plotted in red, while cross-section spectra of various constituent species scaled to the observed quantities are shown below (reactants) and above (products) the data. The colors of the observed spectra match the colors of the boxes in the mechanism shown in Figure 1.

Reference spectra are obtained at the highest possible resolution and then apodized to match the resolution of the data. Spectra in these figures are taken from HITRAN (CF_2O, H_2O, CO_2, NO, NO_2)[13] or are measured on our system (C_3F_6, CF_2O). All spectra, including the data, are high-pass filtered at 128 cm^{-1} for the analysis but not for this plot. The same range is used for the uncertainty analysis. In addition, a region from 1150 to 1350 cm^{-1} is masked out in the analysis because an unidentified product shows significant optical depth there.

Because the only independent parameter changing during the modulation is the flow of hydrogen molecules into the radical source (eq 1), we expect strict conservation of mass for all other atoms, including nitrogen, carbon, and oxygen. We focus first on the nitrogen species. The dominant influence on NO_x is the radical source, which consumes NO_2 and produces mostly NO and a small amount of $HONO_2$ via the reaction of OH with NO_2. The halocarbon oxidation chemistry will tend to drive any NO produced back to NO_2, and it may produce organic nitrates. With the exception of any organic nitrate production, we expect the sum of NO_2, NO, and $HONO_2$ to be zero. Figure 3 shows this expectation to hold, with a mass balance of 0.99 ± 0.08.

With sufficiently high NO and O_2, as in this experiment, we expect the yield of the aldehydes to be near unity. In Figure 3 we show the quantity of C_3F_6 removed and the ratios of the two aldehydes to this quantity. These are the branching ratios of the mechanism, and, as expected, they are very close to unity. Roughly 0.1 of the product remains unidentified, but the residual spectrum shows clear features from 1150 to 1350 cm^{-1}, consistent with the unidentified product if it has a similar cross section to the aldehydes.

As mentioned earlier, alkene (or haloalkene) + OH reactions are notoriously difficult to study with absolute kinetics techniques, especially when the common OH source described by reaction 1 is employed. The results shown here explain those problems. The efficient formation of both aldehyde species strongly suggests that the hydrogen from the hydroxyl radical is rapidly abstracted from an organic radical, producing an aldehyde and the hydroperoxy radical. Given sufficient NO, this will rapidly reform OH. The cycle is catalytic, and a possible rate-limiting step in the cycle, under the conditions of this experiment, is

$$HO_2 + NO \rightarrow OH + NO_2 \qquad (8)$$

The rate constant for this reaction is 8 × 10^{-12} cm3 molecules^{-1} s^{-1}, so in this experiment the HO_2 lifetime was approximately 0.01 s. Given a similar lifetime for OH, up to 5 cycles may have occurred between the radical injector and the White cell. It is not straightforward to compare the column-averaged concentrations measured by the FTIR and the localized LIF measurement. However, we know that the reaction plume is approximately 4 cm wide in the White cell, which is 1/3 the tube diameter, and we may thus deduce core concentrations roughly 3 times as great as the column averages shown. Therefore, roughly 1.5 × 10^{12} molecules cm^{-3} C_3F_6 was

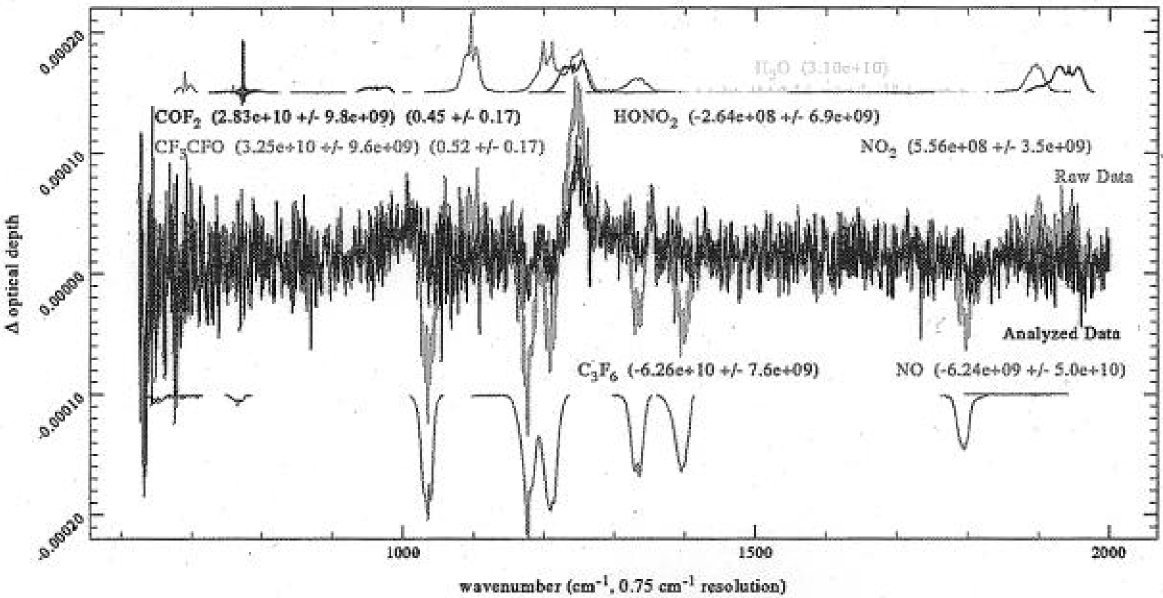

Figure 4. Reaction modulation spectrum for $OH + C_3F_6 \rightarrow$ products with no NO_x present and sharply reduced radical concentrations. The partial production of the aldehydes suggests an $RO_2 + RO_2$ rate constant of $>2 \times 10^{-11}$ cm^3 molecule^{-1} s^{-1}. Analysis for NO_x species indicates their absence and detection limits. The identities of the residual species are not known.

removed from the core of the flow, which is 5 times the initial OH observed.

To investigate the RO_2 radical chemistry in the mechanism, we have performed a series of experiments, most using a second radical source, again initiated by the microwave dissociation of hydrogen:

$$H_2 \rightarrow H + H$$

$$H + O_2 \rightarrow HO_2$$

$$H + HO_2 \rightarrow OH + OH \qquad (9)$$

Under our conditions, OH and HO_2 were generated in roughly equal proportion, which we verified by titrating the HO_2 to OH with added NO. This radical source provides us with great flexibility, since we can either add NO, both converting the HO_2 to OH and encouraging the other RO_2 + NO reactions, or omit the NO and explore $RO_2 + RO_2$ and $RO_2 + HO_2$ reactions.

To reduce the probability of RO_2 radical removal, we reduced the abundance of potential reactants (both other molecules and other RO_2 radicals). Figure 4 shows an RMS spectrum from the experiment with the lowest overall reactivity. The initial radical concentration was roughly a factor of 5 lower than in the experiment shown in Figure 3, and no NO_x was present. To obtain sufficient signal-to-noise, the experiment was run for 12 h. Under these conditions, 0.5 ± 0.2 of the C_3F_6 was converted to the aldehydes, while a correspondingly larger fraction remained in unidentified products, at least some of which are morphologically similar to those seen in Figure 3. In addition to the dominant broad feature at 1250 cm^{-1} and the sharp Q branch at 1275 cm^{-1}, there appear to be absoption features at 1000 and 1350 cm^{-1}. Further experiments are required to identify these products.

The initial radical concentrations (OH and HO_2) in this experiment were roughly 5×10^{11} molecules cm^{-3} in the initial, narrow part of the reaction plume. The White cell was situated some 100 ms downstream of the radical source, so the yield of aldehydes suggests that either the $RO_2 + RO_2$ or the $RO_2 + HO_2$ reaction is very fast ($>2 \times 10^{-11}$), assuming that the RO_2 step is rate limiting.

Conclusions

The data presented here show that the RMS method directly addresses the shortcomings of existing smog chamber experiments. (1) For the test reaction the observed mass balance is 0.99 ± 0.08 for NO_x and 0.86 ± 0.05 for carbon species. The amplitudes of residual features are consistent with the small missing carbon fraction, assuming IR cross sections that are similar to those of the identified aldehyde products. The data for NO_x, in particular where there are no unidentified species in the chemistry and the spectra are well-known, confirm our assertion that the wall-less experiment must conserve mass. (2) Although we have yet to confirm the identity of the spectra observed in the low-reactivity experiments discussed in this paper, the most likely candidates are organoperoxy radicals. This represents the first step of a step-by-step dissection of an oxidation mechanism on a single experiment, with direct observation of all of the species present in the mechanism. (3) The OH radicals that initiate the reaction sequence examined here are rapidly consumed, significantly reducing the probability of complicating side reactions. (4) The low-reactivity experiments were conducted with radical concentrations on the order of 5×10^{11} over 0.1 s and yet show good signal-to-noise. This is very close to the limit where radical−radical reactions in the oxidation sequence will not have time to occur, even at the collision rate. (5) These experiments were conducted at 9 Torr and 300 K. Other experiments have been carried out at pressures up to 700 Torr and temperatures as low as 175 K. The pressure and temperature range of these experiments is simply the pressure and temperature range of the HPF system itself. The RMS technique can thus easily be applied under all conditions found in the atmosphere.

Although the high signal-to-noise shown for the test reaction will be harder to obtain for nonhalogenated hydrocarbons, several relatively easy improvements to our system promise to deliver substantially higher sensitivity to offset the reduced signal. Preliminary experiments on the OH + ethane system clearly show the formation of organic nitrates under conditions similar to those described here. By switching to more sensitive IR detectors (e.g., In:Sb and Si:Ga), in addition to increasing the optical throughput of the experiment, we expect to be able to deliver the signal-to-noise demonstrated here for most hydrocarbon systems. The paradigm for future experiments will be to force an oxidation sequence to completely produce stable oxidation products and then to vary conditions (flows, radical concentrations, etc.) to probe each of the intermediate steps of the mechanism.

Acknowledgment. Several years worth of work along less productive avenues provided the intellectual fuel for this work. We thank in particular our undergraduate assistants, Ted Klupinski and Dalia Trachtenberg, and Michele Sprengnether and her Wellesley assistants, Tara Fortin and Anne Chen. This work was supported by NSF Grant ATM-9414843 to Harvard University, the Empire State Electrical Energy Research Corporation (ESEERCO), and the Electric Power Research Institute (EPRI).

References and Notes

(1) Niki, H.; Maker, P. D. Atmospheric Reactions Involving Hydrocarbons: Long Path-FTIR Studies, *Adv. Photochem*. **1990**, *95*, 5697.

(2) Paukert, T. T.; Johnston, H. S. Spectra and kinetics of the hydroperoxyl free radical in the gas phase. *J. Chem. Phys.* **1971,** *56*, 2824.

(3) Parkes, D. A.; Paul, D. M.; Quinn, C. P. Study of the spectra and recombination kinetics of alkyl radicals by molecular modulation spectrometry. *J. Chem. Soc., Faraday Trans*. **1976,** *72*, 1935.

(4) Burrows, J. P.; Cox, R. A.; Derwent, R. G. Modulated photolysis of the ozone-water vapour system: kinetics of the reaction of OH with HO_2. *J. Photochem*. **1981,** *16*, 147.

(5) Dubey, M. K.; Hannisco, T. F.; Wennberg, P. O.; Anderson, J. G. Monitoring potential photochemical iinterference in laser induced flourescence measurements of atmospheric OH. *Geophys. Res. Lett*., in press.

(6) Stevens, P. S. The HO_2/OH and RO_2/HO_2 ratios during the tropospheric OH photochemistry experiment: measurement and theory. *J. Geophys. Res*., submitted.

(7) Abbatt, J. P. D.; Anderson, J. G. High-pressure discharge flow kinetics and frontier orbital mechanistic analysis for OH + CH_2CCl_2, *cis*-CHClCHCl, *trans*-CHClCHCl, $CFClCF_2$, and CF_2 CCl_2 → products. *J. Phys. Chem*. **1991**, *95*, 2382.

(8) Kuo, C. H.; Lee, Y. P. Kinetics of the reaction OH + C_2H_4 in He, N_2, and O_2 at low pressure. *J. Phys. Chem*. **1991**, *95*, 1253.

(9) Atkinson, R. Gas phase tropospheric chemistry of organic compounds. *J. Phys. Chem. Ref. Data, Monogr*. **1994**, 216.

(10) Abbatt, J. P. D.; Demerjian, K. L.; Anderson, J. G. A new approach to free-radical kinetics: radially and axially resolved high-pressure discharge flow with results for OH + (C_2H_6, C_3H_8, *n*-C_4H_{10}, *n*-C_5H_{12}) → products at 297 K. *J. Phys. Chem*. **1990**, *94*, 4566.

(11) Donahue, N. M.; Clarke, J. S.; Demerjian, K. L.; Anderson, J. G. Free Radical Kinetics at High Pressure: A Mathematical Analysis of the Flow Reactor. *J. Phys. Chem*. **1996,** *100*, 5821.

(12) Wennberg, P. O.; Brault, J. W.; Hanisco, T. F.; Mount, G. H. The Atmospheric Column Abunance of IO: Implications for Stratospheric Ozone. *J. Geophys. Res*., submitted.

(13) Rothman L. S. The Hitran Molecular Database: Editions of 1991 and 1992. *J. Quant. Spectroc. Radiat. Transfer* **1992**, *48*, 469.

JP961393K